

# 3 DIMENSIONAL FIELD CALCULATIONS COMPARED TO MAGNETIC MEASUREMENTS FOR CERN PSB-CPS TRANSFER LINE MAGNETS

M. J. Barnes, G. S. Clark, TRIUMF, M. Sassowsky, CERN

## Abstract

The transfer line PSB-CPS recombines the four beams from the CERN PS Booster (PSB) into one beam, which is injected into the CERN 26 GeV Proton Synchrotron (CPS). As part of the "PS conversion for LHC" project [1], some of the magnets in this transfer line have been replaced by new magnets with laminated yokes and higher maximum current. The magnets were built and magnetically measured by TRIUMF as part of a Canadian contribution to the CERN LHC project. Detailed three dimensional mathematical models have been developed for two types of bending magnets. The models are compared to magnetic measurements and it is shown that the integrated homogeneity curves can be calculated from the 3D model with a precision significantly better than one per mill. The mathematical model is then used to predict the influence of shims on the magnetic field.

## 1 INTRODUCTION

The magnetic field inside an accelerator magnet and sufficiently far from the extremities, can be calculated using a two dimensional field calculation. This assumes that the magnetic vector potential only has a  $z$ -component. To predict the end field correctly, a full three dimensional field calculation is necessary.

The BV1 and BV2 magnets, to be used in the PSB-CPS transfer line, are window frame magnets described in [2] and the references therein. The end fields contribute significantly to  $\int B dl$ . The magnetic measurements [2] were carried out with a 1D Hall probe, which measured only the main component of the field. For the BV1 magnets a characteristic asymmetry caused by the single bedstead coil was found, which could be sufficiently well compensated by adding a shim to the yoke extension block.

A 3D code has been used to simulate BV1 and BV2, and the predictions have been compared with the measurements. The software used for the calculations is Opera-3D [6], which solves the field equations with boundary conditions by finite element discretisation. The non-linear properties of the magnet steel are taken into account by an iterative solution using a Newton-Raphson method.

## 2 MODELLING CONSIDERATIONS

### 2.1 Yoke

The yoke is built from 1.5 mm thick laminations of low carbon steel [5] stacked between two 10 mm thick massive endplates. The effect of the laminations is modelled by

introducing effective permeabilities normal ( $\mu_n$ ) and tangential ( $\mu_t$ ) to the plane of the laminations [3]:

$$\mu_t = s\mu_{steel} + (1 - s) \approx s\mu_{steel} \quad (1)$$

$$\mu_n = \left( \frac{s}{\mu_{steel}} + (1 - s) \right)^{-1} \quad (2)$$

For common values of the stacking factor  $s$  (typically 0.96 to 0.99) and the steel permeability  $\mu_{steel}$  (several thousand), the term  $(1 - s)$  in Eq. 2 dominates. Thus  $\mu_n$  is only weakly dependant upon the steel permeability, and is small compared to  $\mu_t$  and  $\mu_{steel}$ . The physical meaning is that the B field lines are essentially parallel to the laminations. In Opera-3D,  $\mu_n$  and  $\mu_t$  are calculated from the BH curve, the stacking factor and the orientation of the lamination [7].

The longitudinal fringe field originates from the end plates with the field direction essentially normal to the lamination plane. It is therefore essential to include in the model the non-laminated endplate with an isotropic permeability equal to the steel permeability.

### 2.2 Coils

The coils of the BV1 and BV2 magnets are bedstead coils made of 8 circuits with 14 windings each. The coil heads are not identical, as one coil head contains the layer-to-layer transitions and the 16 coil tails for hydraulic and electrical connections. The model uses the GBED coil macro with the shape of the coil heads identical to the actual shape on the non-connection side of the coil. The absolute value of the current density was fine-tuned so that the local B field in the magnet centre is equal to the measured value.

### 2.3 Meshing and potential types

The model was built using hexahedral meshes. The results using a mesh generated with the new automatic tetrahedral mesh generator introduced in version 7 of Opera-3D were found to be not accurate enough. In the  $x$ - $y$ -plane the finest meshing was generated in the centre of the aperture. Several triangular regions (containing degenerate tetrahedral meshes) create transitions to the outside regions with a coarser mesh. An air layer outside the dimensions of the magnet yoke was included to minimise the influence of the outer boundary conditions on the results. In the  $z$ -direction (longitudinal) the models consist of seven layers with the finest mesh size in the layers around the endplate. All regions containing the coil, and the region between the pole faces, are reduced potential regions [8]; the yoke and part of the outer air regions are total potential regions. The total potential regions and the reduced potential regions are topographically singly connected [8]. Fig. 1 shows perspective views of both models.

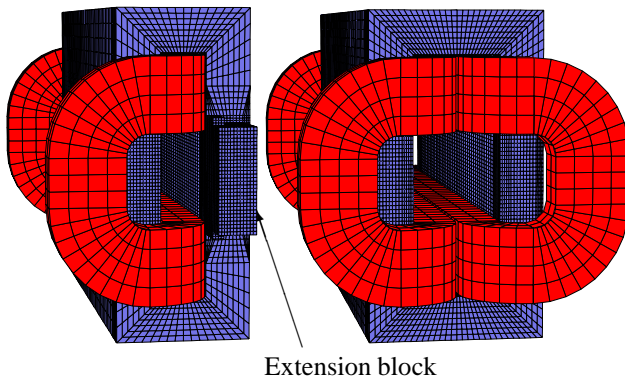
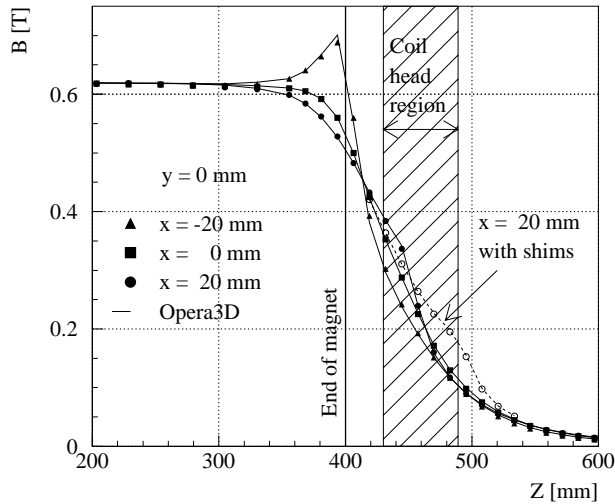


Figure 1: BV1 (left) and BV2 (right)

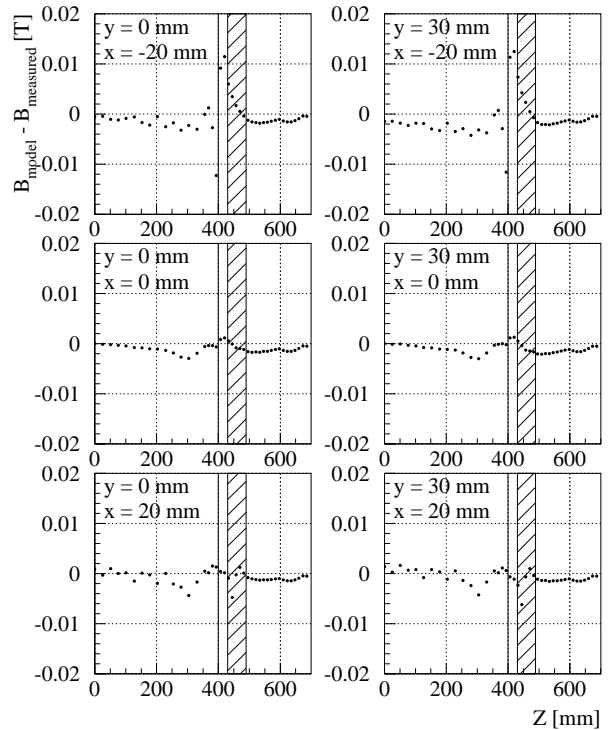

 Figure 2: Measured and calculated  $B_x$  for BV1 #1

### 3 RESULTS

#### 3.1 BV1

Fig. 2 shows the main field component  $B_x$  for BV1 as a function of the longitudinal position in the magnet; points represent the measurements and lines represent the calculations. A pronounced asymmetry caused by the single coil head can be seen. On the side of the coil head ( $x < 0$ ) a maximum of the local field inside the yoke (at  $z \approx 390$  mm) can be seen. The effect of the yoke extension block manifests itself by an increase of the local field for positive  $x$  up to  $z \approx 450$  mm, which corresponds to the actual length of the block in the  $z$ -direction. In general the calculated values correspond well to the measured ones. With shims attached to the yoke extension block, the increase of the local field extends up to  $z \approx 500$  mm.

Fig. 3 shows the difference between measured and calculated values, the largest systematic differences can be seen for negative  $x$  close to the end of the magnet. The RMS spread between the measured and calculated field is  $1.47 \cdot 10^{-3}$  T (without shims) and  $1.43 \cdot 10^{-3}$  T (with shims) [3] which corresponds to 2.3‰ of the central field. Comparing the measurements of BV1 #1 and #2 yields an RMS


 Figure 3: Predicted  $B_x$  - measured  $B_x$  for BV1

difference of  $1.34 \cdot 10^{-3}$  T [3], corresponding to 2.1‰ of the central field. This means that the difference between model and measurements is not significantly larger than the difference between the two magnets.

Fig. 4 compares the measured and calculated homogeneity curves of BV1 #1 without shims and of BV1 #1 and #2 with shims. The predicted and measured values agree to better than one per mill. Again, the difference between measurement and model is not significantly larger than the difference between the measurements of the two magnets. Part of the systematic deviation can be attributed to a slope of the measured curves which is most probably due to a slight non-parallelism (0.1 mm) of the pole faces. On the other hand the model underestimates the curvature of the curve (i.e. sextupolar component) for  $x = -20$  mm.

#### 3.2 BV2

The agreement between measurements and calculations for BV2 is comparable to that reported above for BV1 [3]. The BV2 model is then used to predict the effect of wedge-shaped shims added to the end plate, as proposed in [4], to include a gradient component in the dipolar field.

Fig. 5 shows the end region of the BV2 model with the shims included, seen from the inside of the aperture. Fig. 6 shows the calculated homogeneity curves for three cases, with no shims (top row), with shims of an angle of 50 mrad (middle row) and with shims of an angle of 150 mrad (lower row). The left and right columns show the homogeneity as a function of  $y$  and  $x$ , respectively. The vertical gradient produced by the 50 mrad shim at  $x = 0$  mm is

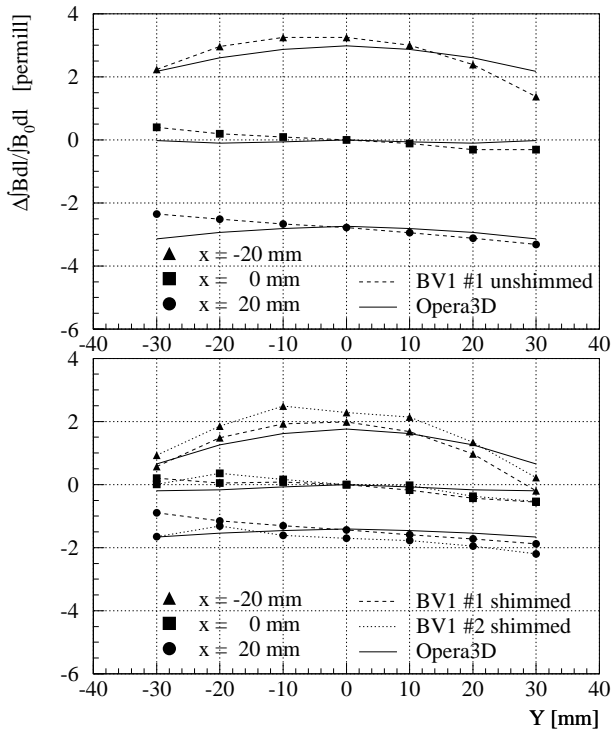


Figure 4: Measured and calculated homogeneity curves

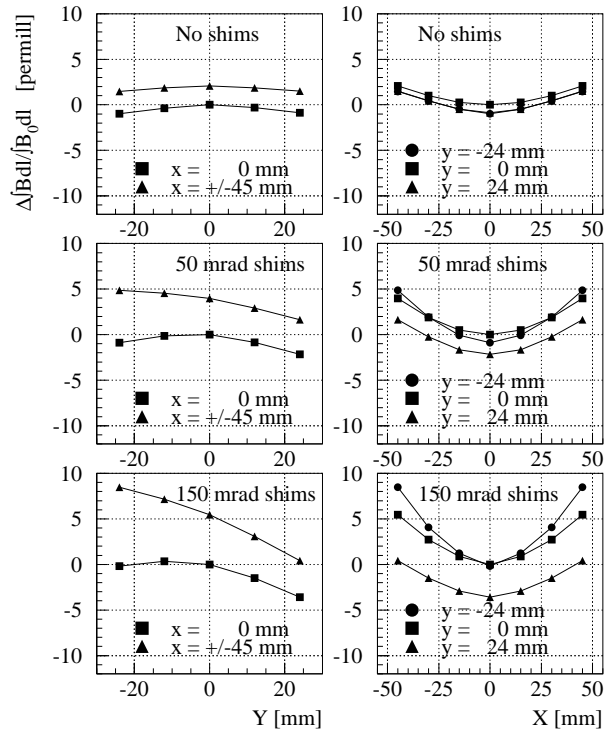


Figure 6: Calculated BV2 homogeneity curves

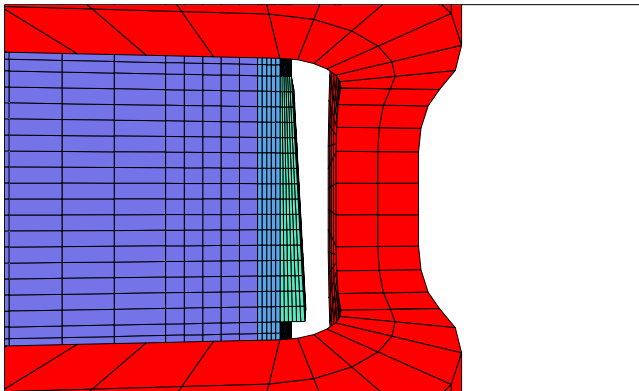


Figure 5: BV2 model with wedge shaped shims

only one third than what would be naively expected. Increasing the shim to an angle of 150 mrad can produce the desired vertical gradient, but creates a much stronger sextupolar component in the horizontal ( $x$ ) direction.

#### 4 CONCLUSIONS

The magnetic field of the BV1 and BV2 transfer line magnets has been calculated using the Opera-3D program. The integrated homogeneity curves can be calculated from the 3D model with a precision significantly better than one per mill. The influence of the BV1 shims is well described by the model. Wedge shaped shims with an angle of 150 mrad added to the BV2 model produce a vertical gradient component proposed in [4], but at the same time a significantly

higher sextupolar component in the horizontal direction.

#### 5 ACKNOWLEDGEMENT

The authors wish to thank D. Evans (TRIUMF) for carrying out the magnetic measurements on the BV1 and BV2 magnets.

#### 6 REFERENCES

- [1] F. Blas et al., Conversion of the PS complex as LHC proton pre-injector, PAC97, Vancouver, Canada, 12-16 May 1997
- [2] M. J. Barnes et al., New magnets for the transfer line PSB-CPS, CERN SL-Note-98-052 MS
- [3] M. J. Barnes, G. S. Clark, M. Sassowsky, Three dimensional field calculations compared to magnetic measurements for BV1 and BV2 transfer line magnets, CERN SL-Note-98-063 MS
- [4] A. Jansson et al., Study of the emittance blow-up sources between the PS Booster and the 26 GeV PS, 1998 European Particle Accelerator Conference (EPAC 98), Stockholm, Sweden, 22-26 June 1998
- [5] Magnetil BC steel, Cockerill Sambre, Seraing, Belgium
- [6] Opera-3D version 7.005, Vector Fields Limited, 24 Bankside, Kidlington, Oxford OX5 1JE, England
- [7] Opera-3D applications notes, VF-01-98-X6
- [8] Opera-3D user guide, VF-01-98-D2, Chapter 2